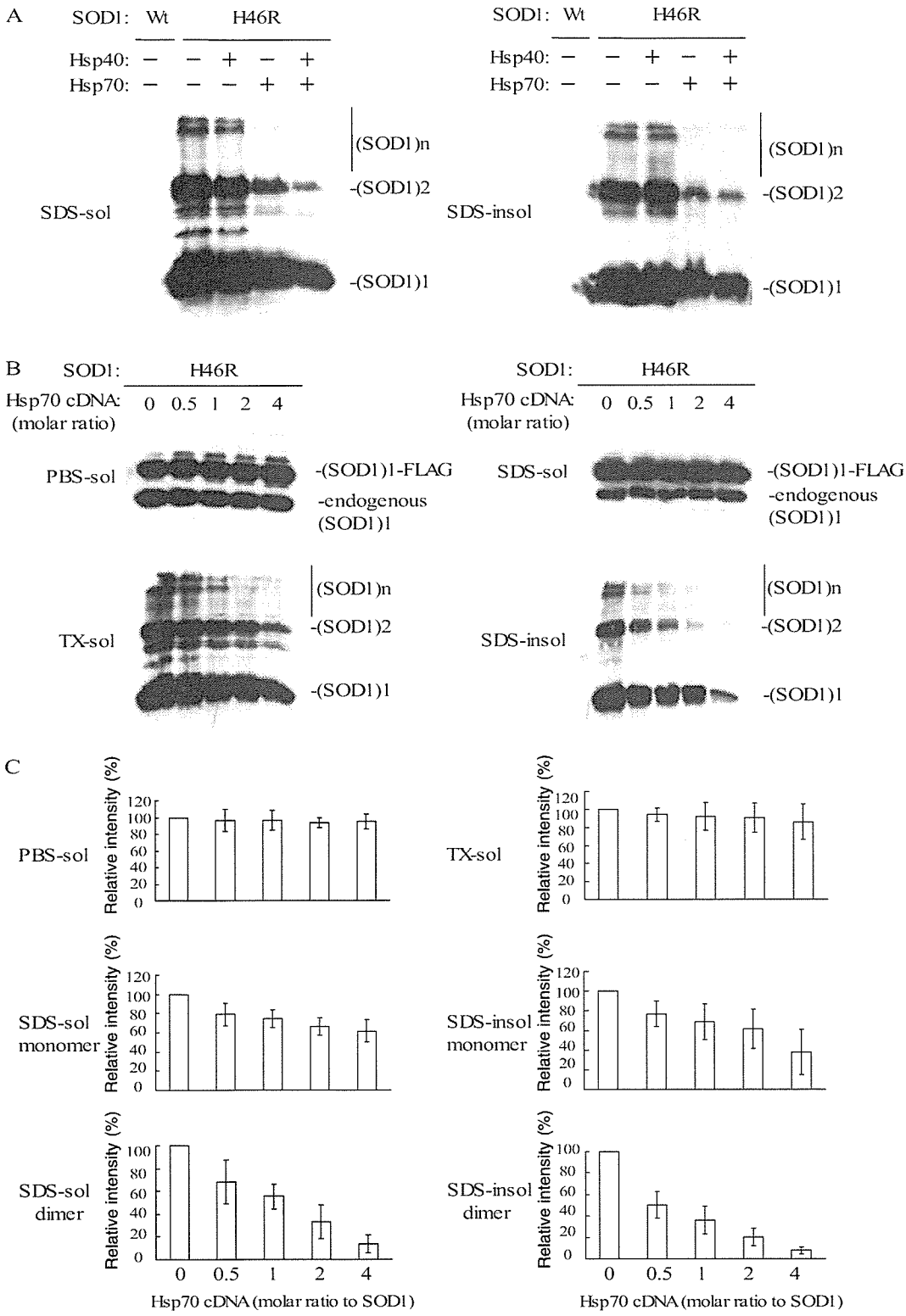

Fig. 5. The effect of overexpression of Hsp70 and Hsp40 on the level of altered insoluble mutant SOD1 in intact cells. (A) Western blots of COS-7 cells co-transfected with H46R SOD1-FLAG pEF-BOS and either pCMV-Hsp70 or pRC-Hsp40 (molar ratio of Hsp versus SOD1 cDNA was 4:1) using SOD1-100 antibody. Proteins from the SDS-soluble (SDS-sol) and SDS-insoluble (SDS-insol) fractions were loaded to the gel and immunoblotted with SOD1-100 antibody. (B) Western blot analysis of cells co-transfected with H46R SOD1-FLAG pEF-BOS and various amounts of Hsp70 cDNA. Molar ratios of pCMV-Hsp70 versus H46R SOD1-FLAG pEF-BOS are indicated in the figure. Forty-eight hours after transfection, cells were harvested and fractionated. Proteins from each fraction were analyzed by Western blotting using an SOD1-100 antibody. (C) The graphs show the relative intensities of H46R SOD1 monomers and dimers in each fraction shown in (B). The relative intensities were quantified by densitometry and normalized to bands from cells transfected with the empty vector (n = 3, bars represent mean ± SD).

size than visible inclusions, and the presence of visible inclusions composed of highly insoluble aggregates contributes less to the early pathological event.

Our findings are relevant to the previous reports that detergent-insoluble dimers and HMW species were found before onset of motor disability and the appearance of pathological SOD1-aggregates in mutant SOD1 transgenic mice [16,19]. However, in these preceding experiments, the alteration of mutant SOD1 solubility was assessed by fractionation using only one detergent. By the sequential extraction of mutant transgenic mouse spinal cords with PBS and TX containing buffer for removing cytosolic and mitochondrial SOD1 with normal solubility equivalent to wild-type SOD1, we separated H46R SOD1 into three different kinds of mutant-specific insoluble species, indicating that insoluble mutant SOD1 did not consist of a uniform species. To see whether SDS-dissociable soluble monomers, in addition to SDS-stable soluble dimers, represented early misfolded intermediates, we have investigated the alteration of SOD1 solubility using a cell culture model of fALS. Treatment with proteasome inhibitors caused the accumulation of SDS-dissociable soluble mutant H46R SOD1 monomers and SDS-stable soluble dimers earlier than that of SDS-stable soluble HMW species and SDS-insoluble species. This finding resembled the age-dependent alteration of SOD1 solubility in mutant H46R SOD1 transgenic mice. In contrast, overexpression of Hsp70 reduced the levels of SDS-dissociable soluble mutant H46R SOD1 monomers and SDS-stable soluble dimers. These findings indicate that SDS-dissociable soluble mutant SOD1 monomers and SDS-stable soluble dimers are degraded by the proteasome pathway and are modulated by molecular chaperones as misfolded intermediates. The previous in vitro study showed that a normal homodimer of SOD1 dissociates to an aggregation-prone monomeric intermediate by oxidation [32]. Further experiments would be necessary to see how potentially aggregation-promoting modifications, such as oxidation and nitration, relate to the alteration of SOD1 solubility.

Several reports showed that Hsp70 and its co-chaperone Hsp40 were involved in the aggregation process or the degradation of SOD1 [11,33], and Hsp70 and Hsp40 suppress SOD1 aggregate formation and improve neurite outgrowth [34]. Although in the previous report up-regulation of Hsp70 was not observed in the spinal cords of mutant SOD1 transgenic mice in contrast to cultured cells overexpressing mutant SOD1 [23], we found that the levels of Hsp70 and Hsp40 in mutant SOD1 transgenic mice increased in the SDS-soluble fraction before disease onset. This observation is consistent with the report that Hsp70 interacts with detergent-insoluble SOD1 rather than detergent-soluble SOD1 in cells [33]. However, it should be noted that endogenous Hsp70 and Hsp40 in the SDS-soluble fraction do not suppress accumulation of insoluble mutant SOD1 in the present H46R SOD1 transgenic mice. Furthermore, Liu et al. [35] showed that elevation of Hsp70 does not affect ALS disease onset and survival in several types of mutant SOD1 transgenic mice co-overexpressing Hsp70 at ~10-fold higher levels than control mice, suggesting that there was no benefit from chronically elevated Hsp70. In cells, overexpression of Hsp70 reduced the levels of SDS-soluble and SDS-insoluble mutant H46R SOD1, whereas it did not lead to the elevation of PBS-soluble and TX-soluble SOD1 levels. This result implies that overexpression of Hsp70 had an effect on the levels of mutant-specific insoluble SOD1 species by forwarding them to the degradation pathway rather than refolding them to a normal soluble pool of SOD1. Adachi et al. [36] reported that overexpression of Hsp70 decreased soluble monomeric androgen receptor (AR) protein in addition to HMW mutant AR protein in double transgenic mice expressing mutant AR protein and Hsp70, suggesting that Hsp70 enhanced mutant AR degradation. Since inhibition of the proteasome activity in cells had a strong effect on the accumulation of insoluble mutant SOD1 with up-regulation of endogenous Hsp70 and Hsp40, the discrepancy in beneficial effects of Hsp70 between cellular and mouse models of fALS may be explained by several possibilities. First, the diminishing of the proteasome activity may generate abundant misfolded proteins whose concentration exceeds the capacity of up-regulated endogenous Hsp70/40. Second, the main function of Hsp70 is to facilitate the proteasome pathway-dependent clearance of misfolded SOD1. Third, the accumulation of insoluble SOD1 species directly impairs the chaperone function of Hsp70 [37]. An approach for examining the toxicity of SDS-dissociable soluble mutant SOD1 monomers and SDS-stable soluble dimers may provide a clue to prevent a further accumulation of potentially toxic misfolded protein complexes in fALS.

Acknowledgments

This work was supported by Research Grants from the Japan ALS association (S.A.), a Grant-in-Aid for Scientific Research on Priority Areas (Advanced Brain Science Project) from the Ministry of Education, Culture, Sports, Science and Technology, Japan (S.A.), and a Research Grant on Measures for Intractable Diseases from the Ministry of Health, Labour and Welfare (T.K.).

References

[1] D.R. Rosen, T. Siddique, D. Patterson, D.A. Figlewicz, P. Sapp, A. Hentati, D. Donaldson, J. Goto, J.P. O'Regan, H.X. Deng, et al., Mutations in Cu/Zn superoxide dismutase gene are associated with familial amyotrophic lateral sclerosis, Nature 362 (1993) 59–62.

[2] M.E. Cudkowicz, D. McKenna-Yasek, P.E. Sapp, W. Chin, B. Geller, D.L. Hayden, D.A. Schoenfeld, B.A. Hosler, H.R. Horvitz, R.H. Brown, Epidemiology of mutations in superoxide dismutase in amyotrophic lateral sclerosis, Ann. Neurol. 41 (1997) 210–221.

[3] J.S. Valentine, P.J. Hart, Misfolded CuZnSOD and amyotrophic lateral sclerosis, Proc. Natl. Acad. Sci. USA 100 (2003) 3617–3622.

[4] A. Okado-Matsumoto, I. Fridovich, Subcellular distribution of superoxide dismutases (SOD) in rat liver: Cu,Zn-SOD in mitochondria, J. Biol. Chem. 276 (2001) 38388–38393.

[5] A.G. Reaume, J.L. Elliott, E.K. Hoffman, N.W. Kowall, R.J. Ferrante, D.F. Siwek, H.M. Wilcox, D.G. Flood, M.F. Beal, R.H. Brown Jr., R.W. Scott, W.D. Snider, Motor neurons in Cu/Zn superoxide dismutase-deficient mice develop normally but exhibit enhanced cell death after axonal injury, Nat. Genet. 13 (1996) 43–47.

[6] M.E. Gurney, H. Pu, A.Y. Chiu, M.C. Dal Canto, C.Y. Polchow, D.D. Alexander, J. Caliendo, A. Hentati, Y.W. Kwon, H.X. Deng, et al., Motor neuron degeneration in mice that express a human Cu,Zn superoxide dismutase mutation, Science 264 (1994) 1772–1775.

[7] M.E. Ripps, G.W. Huntley, P.R. Hof, J.H. Morrison, J.W. Gordon, Transgenic mice expressing an altered murine superoxide dismutase gene provide an animal model of amyotrophic lateral sclerosis, Proc. Natl. Acad. Sci. USA 92 (1995) 689–693.

[8] P.C. Wong, C.A. Pardo, D.R. Borchelt, M.K. Lee, N.G. Copeland, N.A. Jenkins, S.S. Sisodia, D.W. Cleveland, D.L. Price, An adverse property of a familial ALS-linked SOD1 mutation causes motor neuron disease characterized by vacuolar degeneration of mitochondria, Neuron 14 (1995) 1105–1116.

[9] L.I. Bruijn, M.W. Becher, M.K. Lee, K.L. Anderson, N.A. Jenkins, N.G. Copeland, S.S. Sisodia, J.D. Rothstein, D.R. Borchelt, D.L. Price, D.W. Cleveland, ALS-linked SOD1 mutant G85R mediates damage to astrocytes and promotes rapidly progressive disease with SOD1-containing inclusions, Neuron 18 (1997) 327–338.

[10] N. Shibata, A. Hirano, M. Kobayashi, T. Siddique, H.X. Deng, W.Y. Hung, T. Kato, K. Asayama, Intense superoxide dismutase-1 immunoreactivity in intracytoplasmic hyaline inclusions of familial amyotrophic lateral sclerosis with posterior column involvement, J. Neuropathol. Exp. Neurol. 55 (1996) 481–490.

[11] M. Watanabe, M. Dykes-Hoberg, V.C. Culotta, D.L. Price, P.C. Wong, J.D. Rothstein, Histological evidence of protein aggregation in mutant SOD1 transgenic mice and in amyotrophic lateral sclerosis neural tissues, Neurobiol. Dis. 8 (2001) 933–941.

[12] P.A. Jonsson, K. Ernhill, P.M. Andersen, D. Bergemalm, T. Brannstrom, O. Gredal, P. Nilsson, S.L. Marklund, Minute quantities of misfolded mutant superoxide dismutase-1 cause amyotrophic lateral sclerosis, Brain 127 (2004) 73–88.

[13] H.D. Durham, J. Roy, L. Dong, D.A. Figlewicz, Aggregation of mutant Cu/Zn superoxide dismutase proteins in a culture model of ALS, J. Neuropathol. Exp. Neurol. 56 (1997) 523–530.

[14] T. Koide, S. Igarashi, K. Kikugawa, R. Nakano, T. Inuzuka, M. Yamada, H. Takahashi, S. Tsuji, Formation of granular cytoplasmic aggregates in COS7 cells expressing mutant Cu/Zn superoxide dismutase associated with familial amyotrophic lateral sclerosis, Neurosci. Lett. 257 (1998) 29–32.

[15] M. Nagai, M. Aoki, I. Miyoshi, M. Kato, P. Pasinelli, N. Kasai, R.H. Brown Jr., Y. Itoyama, Rats expressing human cytosolic copper-zinc superoxide dismutase transgenes with amyotrophic lateral sclerosis: associated mutations develop motor neuron disease, J. Neurosci. 21 (2001) 9246–9254.

[16] J.A. Johnston, M.J. Dalton, M.E. Gurney, R.R. Kopito, Formation of high molecular weight complexes of mutant Cu, Zn-superoxide dismutase in a mouse model for familial amyotrophic lateral sclerosis, Proc. Natl. Acad. Sci. USA 97 (2000) 12571–12576.

[17] K. Puttaparthi, C. Wojcik, B. Rajendran, G.N. DeMartino, J.L. Elliott, Aggregate formation in the spinal cord of mutant SOD1 transgenic mice is reversible and mediated by proteasomes, J. Neurochem. 87 (2003) 851–860.

[18] J. Wang, G. Xu, D.R. Borchelt, High molecular weight complexes of mutant superoxide dismutase 1: age-dependent and tissue-specific accumulation, Neurobiol. Dis. 9 (2002) 139–148.

[19] M. Urushitani, J. Kurisu, K. Tsukita, R. Takahashi, Proteasomal inhibition by misfolded mutant superoxide dismutase 1 induces selective motor neuron death in familial amyotrophic lateral sclerosis, J. Neurochem. 83 (2002) 1030–1042.

[20] S. Tobisawa, Y. Hozumi, S. Arawaka, S. Koyama, M. Wada, M. Nagai, M. Aoki, Y. Itoyama, K. Goto, T. Kato, Mutant SOD1 linked to familial amyotrophic lateral sclerosis, but not wild-type SOD1, induces ER stress in COS7 cells and transgenic mice, Biochem. Biophys. Res. Commun. 303 (2003) 496–503.

[21] D.H. Hyun, M. Lee, B. Halliwell, P. Jenner, Proteasomal inhibition causes the formation of protein aggregates containing a wide range of proteins, including nitrated proteins, J. Neurochem. 86 (2003) 363–373.

[22] E. Kabashi, J.N. Agar, D.M. Taylor, S. Minotti, H.D. Durham, Focal dysfunction of the proteasome: a pathogenic factor in a mouse model of amyotrophic lateral sclerosis, J. Neurochem. 89 (2004) 1325–1335.

[23] W. Bruening, J. Roy, B. Giasson, D.A. Figlewicz, W.E. Mushynski, H.D. Durham, Up-regulation of protein chaperones preserves viability of cells expressing toxic Cu/Zn-superoxide dismutase mutants associated with amyotrophic lateral sclerosis, J. Neurochem. 72 (1999) 693–699.

[24] C.A. Ross, M.A. Poirier, Protein aggregation and neurodegenerative disease, Nat. Med. 10 (Suppl.) (2004) S10–S17.

[25] A.A. Michels, B. Kanon, A.W. Konings, K. Ohtsuka, O. Bensaude, H.H. Kampinga, Hsp70 and Hsp40 chaperone activities in the cytoplasm and the nucleus of mammalian cells, J. Biol. Chem. 272 (1997) 33283–33289.

[26] Y. Kobayashi, A. Kume, M. Li, M. Doyu, M. Hata, K. Ohtsuka, G. Sobue, Chaperones Hsp70 and Hsp40 suppress aggregate formation and apoptosis in cultured neuronal cells expressing truncated androgen receptor protein with expanded polyglutamine tract, J. Biol. Chem. 275 (2000) 8772–8778.

[27] S. Arawaka, H. Hasegawa, A. Tandon, C. Janus, F. Chen, G. Yu, K. Kikuchi, S. Koyama, T. Kato, P.E. Fraser, P. St. George-Hyslop, The levels of mature glycosylated nicastrin are regulated and correlate with gamma-secretase processing of amyloid beta-precursor protein, J. Neurochem. 83 (2002) 1065–1071.

[28] R. Chang-Hong, M. Wada, S. Koyama, H. Kimura, S. Arawaka, T. Kawanami, K. Kurita, T. Kadoya, M. Aoki, Y. Itoyama, T. Kato, Neuroprotective effect of oxidized galectin-1 in a transgenic mouse model of amyotrophic lateral sclerosis, Exp. Neurol. 194 (2005) 203–211.

[29] C.J. Epstein, K.B. Avraham, M. Lovett, S. Smith, O. Elroy-Stein, G. Rotman, C. Bry, Y. Groner, Transgenic mice with increased Cu/Zn-superoxide dismutase activity: animal model of dosage effects in Down syndrome, Proc. Natl. Acad. Sci. USA 84 (1987) 8044–8048.

[30] H. Fujiwara, M. Hasegawa, N. Dohmae, A. Kawashima, E. Masliah, M.S. Goldberg, J. Shen, K. Takio, T. Iwatsubo, alpha-Synuclein is phosphorylated in synucleinopathy lesions, Nat. Cell. Biol. 4 (2002) 160–164.

[31] P.J. Kahle, M. Neumann, L. Ozmen, V. Muller, S. Odoy, N. Okamoto, H. Jacobsen, T. Iwatsubo, J.Q. Trojanowski, H. Takahashi, K. Wakabayashi, N. Bogdanovic, P. Riederer, H.A. Kretzschmar, C. Haass, Selective insolubility of alpha-synuclein in human Lewy body diseases is recapitulated in a transgenic mouse model, Am. J. Pathol. 159 (2001) 2215–2225.

[32] R. Rakhit, J.P. Crow, J.R. Lepock, L.H. Kondejewski, N.R. Cashman, A. Chakrabartty, Monomeric Cu,Zn-superoxide dismutase is a common misfolding intermediate in the oxidation models of sporadic and familial amyotrophic lateral sclerosis, J. Biol. Chem. 279 (2004) 15499–15504.

[33] G.A. Shinder, M.C. Lacourse, S. Minotti, H.D. Durham, Mutant Cu/Zn-superoxide dismutase proteins have altered solubility and interact with heat shock/stress proteins in models of amyotrophic lateral sclerosis, J. Biol. Chem. 276 (2001) 12791–12796.

[34] H. Takeuchi, Y. Kobayashi, T. Yoshihara, J. Niwa, M. Doyu, K. Ohtsuka, G. Sobue, Hsp70 and Hsp40 improve neurite outgrowth and suppress intracytoplasmic aggregate formation in cultured neuronal cells expressing mutant SOD1, Brain Res. 949 (2002) 11–22.

[35] J. Liu, L.A. Shinobu, C.M. Ward, D. Young, D.W. Cleveland, Elevation of the Hsp70 chaperone does not effect toxicity in mouse

models of familial amyotrophic lateral sclerosis, J. Neurochem. 93 (2005) 875–882.
[36] H. Adachi, M. Katsuno, M. Minamiyama, C. Sang, G. Pagoulatos, C. Angelidis, M. Kusakabe, A. Yoshiki, Y. Kobayashi, M. Doyu, G. Sobue, Heat shock protein 70 chaperone overexpression ameliorates phenotypes of the spinal and bulbar muscular atrophy transgenic mouse model by reducing nuclear-localized mutant androgen receptor protein, J. Neurosci. 23 (2003) 2203–2211.
[37] H. Tummala, C. Jung, A. Tiwari, C.M. Higgins, L.J. Hayward, Z. Xu, Inhibition of chaperone activity is a shared property of several Cu,Zn-superoxide dismutase mutants that cause amyotrophic lateral sclerosis, J. Biol. Chem. 280 (2005) 17725–17731.

JBC Papers in Press. Published on March 2, 2006 as Manuscript M513552200
The latest version is at http://www.jbc.org/cgi/doi/10.1074/jbc.M513552200

CALCIUM SENSING RECEPTOR UBIQUITINATION AND DEGRADATION MEDIATED BY THE E3 UBIQUITIN LIGASE DORFIN

Ying Huang[1,3], Jun-ichi Niwa[2], Gen Sobue[2] and Gerda E. Breitwieser[3]*

From the *Department of Biology, Syracuse University, Syracuse, NY 13244; # Department of Neurology, Nagoya University Graduate School of Medicine, Nagoya 466-8500, Japan; and †Weis Center for Research, Geisinger Clinic, Danville PA 17822

*Address correspondence to: Gerda E. Breitwieser, Weis Center for Research, Geisinger Clinic, 100 N. Academy Avenue, Danville, PA, 17822-2604. Phone: (570) 271-6675, Fax: (570) 271-5886; E-mail: gebreitwieser@geisinger.edu.

Running Title: *Dorfin-mediated Calcium Sensing Receptor Degradation*
Key words: Calcium sensing receptor, dorfin, ubiquitination, endoplasmic reticulum-associated degradation pathway, proteasome, protein degradation

Calcium-sensing receptors (CaR) contribute to regulation of systemic calcium homeostasis by activation of G_q- and G_i-linked signaling pathways in the parathyroids, kidney, and intestine. Little is known about the mechanisms regulating CaR synthesis and degradation. Screening of a human kidney yeast two-hybrid library identified the E3 ubiquitin ligase dorfin as a binding partner for the intracellular carboxyl terminus of CaR. Interaction between CaR and dorfin was confirmed by coimmunoprecipitation from HEK293 cells. Ubiquitination of CaR was observed in the presence of the proteasomal inhibitor MG132; mutation of all putative intracellular loop and carboxyl terminal lysine residues abolished ubiquitination of CaR. Coexpression with dorfin decreased the amount of total CaR protein and increased CaR ubiquitination, while a dominant negative fragment of dorfin had opposite effects. The AAA-ATPase p97/valosin-containing protein (VCP) associates with both CaR and dorfin in HEK293 cells. Treatment with tunicamycin, an inhibitor of N-linked glycosylation, induced the appearance of the unglycosylated 115 kD CaR form, which was further increased by exposure to MG132, or upon transfection with a dorfin dominant negative construct, suggesting that dorfin-mediated proteasomal degradation of immature CaR occurs from the endoplasmic reticulum. Since endogenous CaR in MDCK cells is also subject to degradation from the endoplasmic reticulum, dorfin-mediated ubiquitination may contribute to a general mechanism for CaR quality control during biosynthesis.

The calcium sensing receptor (CaR) contributes to maintenance of systemic Ca^{2+} homeostasis, regulating parathyroid hormone secretion, absorption/resorption of Ca^{2+} by the intestine and kidney, and may also have effects in bone (1). CaR belongs to family C of the GPCR

superfamily, having structural similarities to metabotropic glutamate receptors, $GABA_B$ receptors, and some putative pheromone/taste receptors (1,2). Common to all members of family C is a large extracellular domain of more than 600 amino acids containing the agonist binding site, a heptahelical transmembrane domain, and a large intracellular carboxyl terminal tail of more than 200 amino acids (1,2). Members of Family C, including CaR, function as dimers, stabilized either by a disulfide bond or non-covalent interactions (3,4,5). The CaR extracellular domain contains N-linked glycosylation sites (2,6,7), and is stabilized by multiple intramolecular disulfide bonds, as well as one intermolecular disulfide bond between monomers in the dimer (8,9,10). Upon agonist stimulation, CaR activates diverse signaling pathways leading to changes in hormone secretion, cell proliferation, differentiation and/or apoptosis (1). While considerable progress has been made in understanding the structure, activation, and signaling of CaR, the biosynthesis, trafficking, targeting and turnover mechanisms regulating CaR remain largely unexplored.

To identify novel proteins that might regulate trafficking and/or targeting of CaR, the intracellular carboxyl terminus of CaR was used as bait in a yeast two-hybrid (Y2H) screen of a human kidney cDNA library. One of the proteins identified in the screen was the E3 ubiquitin ligase dorfin (double-RING finger protein) (11). Dorfin was originally cloned from human spinal cord and is expressed in many organs, including kidney, liver, intestine, and the central nervous system (11). Dorfin localizes to a region near the centrosome in an aggresome-like structure in cultured cells (11). In the nervous system, dorfin ubiquitinates superoxide dismutase-1 (12) and synphilin-1 (13), and is a component of Lewy bodies observed in Parkinson's and other neurodegenerative diseases (12,13,14). Ubiquitination results in the attachment of ubiquitin, a highly conserved 76-amino acid polypeptide, to the ε-amino group of lysine residues of target proteins, and requires the sequential actions of three enzymes. Final transfer of activated ubiquitin to target proteins is coordinated by the E3 ligase, which specifically interacts with both E2-ubiquitin and the target protein (15). Dorfin contains two RING domains at its amino terminus, which function as recruiting motifs for specific E2s (11). The carboxyl terminus of dorfin has no identifiable motifs, but has been shown to confer specificity of binding to synphilin-1 (13). Dorfin interacts directly with VCP (valosin-containing protein, also called p97 or Cdc48 homologue) (14), an AAA-ATPase proposed to have a role in endoplasmic reticulum-associated protein degradation (ERAD). VCP assists in translocation of ubiquitinated proteins from the ER and acts as a chaperone, targeting ubiquitinated proteins to the proteasome for degradation (16,17,18,19).

In this report, we characterize the functional interactions between CaR and dorfin in HEK293 cells, and demonstrate that dorfin mediates CaR ubiquitination, leading to degradation by the proteasome. Both dorfin and CaR interact with VCP in HEK293 cells, and a dominant negative fragment of dorfin protects immature forms of CaR from degradation. Finally, endogenous CaR in MDCK cells is also

subject to ER-associated degradation, suggesting a common mechanism may regulate quality control of both exogenously and endogenously expressed CaR. These results suggest that dorfin may recognize misfolded or non-functional CaR at the endoplasmic reticulum, leading to ubiquitination and proteasomal degradation.

EXPERIMENTAL PROCEDURES

Materials. Human kidney cDNA library and all the materials for the Y2H screen were purchased from Clontech. HEK293 and MDCK cells were from the American Tissue Culture Collection and used through lab passage number 30. Restriction enzymes were from New England Biolabs and Promega. The EGFP-dorfin plasmid (dorfin chimera with EGFP at amino terminus) and rabbit polyclonal antibody against dorfin (D-30) were generated as described (11). The HA-ubiquitin plasmid was generously provided by Dr. Richard JH Wojcikiewicz (SUNY Upstate Medical University, Syracuse, NY). Monoclonal antibodies were from various sources (anti-Flag M2 and anti-actin antibodies, Sigma; anti-HA antibody, Roche Diagnostics; anti-VCP antibody, Research Diagnostics; anti-GFP antibody, Molecular Probes). Rabbit polyclonal antibody against CaR (LRG) was generated as described (20). Anti-phospho-ERK1/2 (p42/44) polyclonal antibody was from Cell Signaling Technology. ECL anti-mouse and anti-rabbit, horseradish peroxidase-conjugated secondary antibodies were purchased from Amersham. MG132 and tunicamycin were purchased from Sigma.

Plasmid construction. CaR with an amino terminal Flag epitope (Flag-CaR) was generated as described (21). CaR carboxyl terminal (CaR-CT) fragments in the Y2H bait vector pGBKT7 were prepared by PCR using primers containing NdeI and SalI sites, using Flag-CaR as template. PCR products were digested with NdeI/SalI, and subcloned into NdeI/SalI-digested pGBKT7. Dorfin carboxyl terminal fragments in the Y2H prey vector pACT2 were prepared similarly, using NcoI and XhoI sites. The dominant negative construct of dorfin was generated as a chimera with EGFP at the carboxyl terminus (DCT-EGFP). The DCT fragment containing dorfin residues 561-838 was prepared by PCR using primers containing BglII and SalI sites. The PCR product was digested with BglII/SalI and subcloned into BglII/SalI-digested PEGFP-N1 vector (Clontech). Another version of dominant negative dorfin (DCT-*c-myc*) was prepared similarly by PCR the DCT fragment using primers containing XbaI and HindIII sites. The PCR product was digested with XbaI/HindIII and subcloned into XbaI/HindIII-digested pcDNA3.1A(-) vector (Clontech). Another construct of dorfin (DNT-EGFP) containing the N-terminal RING-finger domains of dorfin from residue 1-367 was prepared by PCR using primers containing SacI and KpnI sites. The PCR product was digested with SacI/KpnI and subcloned into SacI/KpnI-digested pEGFP-N1 vector (Clontech). Point mutations were generated by a modified inverse PCR mutagenesis method (22). All PCR reactions used *Pfu* DNA polymerase (Stratagene). All constructs were verified by dideoxy-DNA sequencing (DNA Sequencing Facility, Cornell University, Ithaca, NY). Sequences of primers

provided upon request.

Y2H assay screening. Gal4-based Y2H library screening was performed by yeast mating as recommended in the manufacturer's instructions (Clontech). Yeast *Saccharomyces cerevisiae* MATa strain AH109 was transformed with bait plasmid containing CaR-CT (aa 866-1078) and incubated with yeast *Saccharomyces cerevisiae* MATα strain Y187 pretransformed with human kidney cDNA library (Clontech) in 2xYPDA/Kan at 30°C for 24 hours. The mixture was plated on SD/-Ade/-His/-Leu/-Trp plates to screen for $ADE2^+$ and $HIS3^+$ clones. Plates were incubated at 30 °C until colonies appeared. Colonies were restreaked on SD/-Ade/-His/-Leu/-Trp + X-α-gal plates to screen for $MEL1^+$ clones. Clones that activated three reporter genes, ADE2, HIS3 and MEL1, were considered positive and identified by purifying plasmids and sequencing inserts.

Directed Y2H studies were performed by cotransformation using the lithium acetate method (23). Bait plasmids containing CaR-CT fragments and prey plasmids containing dorfin carboxyl terminal fragments were cotransformed into AH109 and plated on SD/-Ade/-His/-Leu/-Trp + X-α-gal plates. An interaction was considered positive when three reporter genes (ADE2, HIS3 and MEL1) were activated.

Cell culture and transfection. HEK293 and MDCK cells were grown in high glucose Dulbecco's modified Eagle's medium (DMEM), supplemented with 10% heat-inactivated fetal calf serum, 50 units/ml penicillin, and 50 μg/ml streptomycin (37 °C, 5% CO_2). HEK293 cells were transiently transfected with Novafector (Venn Nova LLC, Pompano, FL) according to manufacturer's instructions; experiments were done seventy-two hours after transfection. For inhibitor studies, cells were treated with MG132 and/or tunicamycin (solubilized in DMSO) for twelve hours prior to lysis. Comparable levels of DMSO had no effect on measured parameters.

SDS-PAGE and western blotting. Transfected HEK293 cells or MDCK cells were washed with PBS-EDTA and lysed on ice with PBS containing 5 mM EDTA, 0.5% Triton X-100, 10 mM iodoacetamide, plus protease inhibitor mixture (Roche Applied Science). Cell lysates were agitated for 30 min at 4°C and cleared by centrifugation. Supernatants were mixed with loading buffer (12 M urea, 4% SDS, 0.01% bromophenol blue, 100 mM β–mercaptoethanol in 200 mM Tris) and separated on 4-15% SDS-polyacrylamide gels (Bio-Rad) before transfer to nitrocellulose membranes (Bio-Rad). Membranes were incubated with primary antibodies (GFP, 1:500; LRG, 1:1000; HA, 1:1000; actin, 1:1000; D-30, 1:3000; or VCP, 1:1000) overnight at 4°C. Membranes were incubated with secondary antibody coupled to horseradish peroxidase (1:5000) at room temperature for one hour. Proteins were visualized by enhanced chemiluminescence (Super West Pico Chemiluminescent Substrate, Pierce). Assay of ERK1/2 phosphorylation was as previously described (21). When the same blot was probed for the presence of coprecipitated proteins, nitrocellulose membranes were stripped in Restore Western Blot Stripping Buffer (Pierce) and probed with a second primary antibody.

Immunoprecipitation. Transfected HEK293 cells were washed with PBS and lysed as described. After sonication on ice, samples were agitated for 30 min at 4°C and incubated with 10 µl protein G-agarose (Invitrogen) to minimize nonspecific binding. Samples were centrifuged and supernatants incubated with antibody for 3 hrs at 4°C. 15 µl protein G-agarose was then added, and samples rotated overnight (4°C). Precipitates were incubated in loading buffer for 30 min at (25°C), and run on SDS-polyacrylamide gels as described. To detect specific ubiquitination, a two-step immunoprecipitation was performed. After the first immunoprecipitation as described, pellets were washed three times with lysis buffer and incubated with 1% SDS/PBS for 30 minutes (25°C) to disrupt non-covalent interactions. Samples were centrifuged and supernatants were diluted with lysis buffer, followed by a second immunoprecipitation. The resultant precipitates were incubated in loading buffer and separated on SDS-polyacrylamide gels as described.

Densitometry and statistics. Blots were digitized using an Epson Expression 800 Photo scanner and quantified by densitometry using AlphaEaseFC StandAlone Software (San Leandro, CA). Results were mean ± S.D. of at least three independent experiments; graphs were generated using Sigma Plot 2000. Student's t-test (two comparisons) was performed, $p < 0.05$ was considered significant.

RESULTS

Y2H screen identifies the E3 ubiquitin ligase dorfin as a CaR-binding protein. The cytoplasmic carboxyl terminus of CaR (CT, residues 866-1078) was used as bait to screen a human kidney cDNA library (Figure 1A). Positive clones were selected by activation of three reporter genes, ADE2, HIS3, and MEL1. Blast searches of the NCBI database with positive clones identified in the screen yielded a fragment corresponding to the carboxyl terminus (residues 561-838) of the E3 ubiquitin ligase dorfin (double-RING finger protein), an 838 amino acid protein (Figure 1B) (11).

To localize the dorfin interaction site on the CaR carboxyl terminus, various truncations of the CaR carboxyl terminus (in pGBKT7), illustrated in Figure 1A, were screened against the carboxyl terminus of dorfin (residues 561-838) (in pACT2) after cotransformation in the AH109 strain. The full CaR-CT (residues 866-1078) interacted with dorfin, confirming the results of the initial screen. Truncations of the carboxyl end of CaR-CT were well tolerated, displaying positive interactions with dorfin. Only the smallest fragment, containing residues 866-886, did not interact with dorfin. Truncations from the amino terminus of the CaR-CT narrowed the region for interaction with dorfin to residues 880-900 (Figure 1A).

Complementary directed Y2H screens were performed to localize the CaR-CT interaction site on the carboxyl terminus of dorfin (residues 561-838). Any truncations from the carboxyl terminus of dorfin inhibited interactions with CaR-CT, while interaction with CaR-CT was retained upon removal of up to 100 residues from the amino terminus of the dorfin fragment (residues 561-660). The minimal fragment of the dorfin carboxyl

terminus required for interaction with CaR-CT contains residues from 660-838 (Figure 1B).

Coimmunoprecipitation of CaR and dorfin from HEK293 cells confirms their interaction. Human CaR having an amino terminal Flag epitope (Flag-CaR) was transfected into HEK293 cells, and Flag-CaR was immunoprecipitated with anti-Flag antibody. The immunoprecipitate was separated on a 4-15% SDS-PAGE reducing gel, blotted to nitrocellulose and probed with anti-dorfin antibody D-30. Endogenous dorfin was observed as a doublet with molecular weight approximately 100 kD in the presence (lane 1) but not in the absence (lane 2) of transfected Flag-CaR (Figure 2A, top panel). The two lower panels in Figure 2 illustrate the expression of endogenous dorfin (probed with anti-dorfin antibody D-30) or Flag-CaR (probed with anti-CaR LRG antibody) in cell lysates. These results confirm the interaction of full length CaR and dorfin in HEK293 cells.

To confirm that the dorfin fragment identified in the Y2H studies is required for the interaction of dorfin and CaR in mammalian cells, Flag-CaR and full length dorfin (EGFP-dorfin) or dorfin truncations (DNT-EGFP or DCT-EGFP) were tested for coimmunoprecipitation from HEK293 cells. DNT-EGFP contains the amino terminal RING-finger domains of dorfin from residue 1-367; DCT-EGFP contains the carboxyl terminal domain of dorfin from residue 561-838. Anti-Flag antibody was used to immunoprecipitate Flag-CaR, and blots were probed with anti-GFP antibody to detect dorfin species. EGFP-dorfin (130 kDa) and DCT-EGFP (60 kDa) coprecipitated with Flag-CaR (Figure 2B, top panel), but DNT-EGFP (68 kDa) did not. Middle and bottom panels of Figure 2B illustrate expression of the indicated constructs in cell lysates when probed with anti-GFP (middle) or anti-CaR LRG (bottom) antibodies. These results confirm that the domain of dorfin mediating the interaction with CaR in yeast, i.e., the carboxyl terminus, is also required for the interaction of dorfin with CaR in mammalian cells.

CaR is ubiquitinated. Interaction between CaR and dorfin suggests that CaR may be ubiquitinated. To test this possibility, Flag-CaR and amino terminal HA-tagged ubiquitin (HA-Ub) were cotransfected into HEK293 cells, and a two-step, denaturing protocol was used to immunoprecipitate Flag-CaR. Briefly, anti-Flag antibody was used to immunoprecipitate CaR, followed by treatment of the pellet with 1% SDS/PBS to disrupt non-covalent interactions between CaR and its associated proteins. The supernatant was diluted with lysis buffer and subjected to a second round of immunoprecipitation with anti-Flag antibody. The western blot was probed with anti-HA antibody to detect ubiquitinated species. Ubiquitination of CaR was observed in the presence of the proteasomal inhibitor MG132, appearing in the range from 150 kD to more than 250 kD, while ubiquitination was barely detectable in the absence of MG132 (Figure 3A, upper panel, lanes 1-2). MG132 increased the amount of CaR protein (Figure 3A, lower panel, lanes 1-2), suggesting that ubiquitination followed by proteasomal degradation contributes to regulation of CaR.

Ubiquitin ligases covalently conjugate ubiquitin to lysine residues of target

proteins. To confirm that CaR is ubiquitinated, we mutated intracellular lysine residues to arginine. There are nine lysine residues within the CaR carboxyl terminus (residues 863, 882, 897, 917, 931, 963, 965, 984 and 1002) and seven lysine residues within the three intracellular loops (residues 636, 644, 709, 717, 793, 796 and 805). When each lysine residue was mutated to arginine individually, the resulting mutants were still heavily ubiquitinated (data not shown). Since single point mutations did not abolish ubiquitination, CaR must be ubiquitinated at more than one lysine residue. All sixteen lysine residues were therefore mutated to arginine simultaneously, and ubiquitination of the mutant, termed Flag-CaR(0K), determined in the absence or presence of MG132 (Figure 3A, upper panel, lanes 3-4). Flag-CaR(0K) was not ubiquitinated to a significant extent even in the presence of MG132. In addition, the amount of Flag-CaR(0K) was not significantly changed upon addition of MG132 (100% in the absence versus 107.6 ± 10.7% in the presence of MG132) (Figure 3A, lower panel, lanes 3-4), while wild type Flag-CaR was sensitive to MG132 treatment (100% in the absence versus 148.4 ± 4.7% in the presence of MG132) (Figure 3A, lower panel, lanes 1-2). Both Flag-CaR and Flag-CaR(0K) achieved mature glycosylation consistent with plasma membrane localization (Figure 3A, lower panel) (6,7), and had a comparable ability to stimulate ERK1/2 phosphorylation upon exposure of cells to 5 mM Ca^{2+} (Figure 3B). The absence of Flag-CaR(0K) ubiquitination is not the result of an inability to associate with dorfin, since immunoprecipitation with anti-Flag antibody of either Flag-CaR or Flag-CaR(0K) results in coprecipitation of comparable levels of endogenous dorfin (Figure 3C, top panel). Also illustrated in Figure 3C is the presence of endogenous dorfin (middle panel) or transfected Flag-CaR (bottom panel) in cell lysates. These results confirm that CaR is ubiquitinated at multiple lysine residues and degraded by the proteasome.

Dorfin mediates CaR ubiquitination. Dorfin is an E3 ubiquitin ligase and interacts with CaR, and therefore likely mediates CaR ubiquitination. To test this possibility, Flag-CaR and HA-Ub cDNAs were cotransfected into HEK293 cells, without or with EGFP-dorfin cDNA. Anti-Flag antibody was used to immunoprecipitate CaR; western blots were probed with anti-HA antibody to detect ubiquitinated species. In the absence of dorfin, a low level of CaR ubiquitination was detected; cotransfection with dorfin dramatically increased CaR ubiquitination (Figure 4A). HEK293 cells express endogenous dorfin (data not shown, but see eg. Figure 2A or 3C), and thus basal CaR ubiquitination (in the absence of cotransfected dorfin) might be catalyzed by endogenous dorfin. To test this possibility, we used DCT-EGFP as a dominant negative to interfere with ubiquitination mediated by endogenous dorfin. This construct cannot catalyze ubiquitination of substrates, since it does not contain the amino terminal RING domains which are essential for interaction with ubiquitin-conjugating enzymes (11). Cotransfection of HEK293 cells with Flag-CaR, HA-Ub and DCT-EGFP resulted in a reduction in CaR ubiquitination, compared with ubiquitination mediated by endogenous dorfin (-DCT) (Figure 4B). These results suggest that the E3 ubiquitin ligase dorfin

mediates ubiquitination of CaR.

Dorfin regulates the amount of CaR protein in HEK293 cells. Since dorfin mediates CaR ubiquitination, it must contribute to regulation of total cellular CaR protein. Flag-CaR cDNA was transfected into HEK293 cells with increasing amounts of EGFP-dorfin cDNA (Figure 5A). Total cDNA was kept constant with pcDNA3.1. The expression of CaR and dorfin were characterized by immunoblotting lysates from HEK293 cells with either anti-CaR LRG antibody (Figure 5A, top blot) or anti-GFP antibody (Figure 5A, bottom blot). Actin was used as a loading control (Figure 5A, middle blot). When dorfin was increased, the amount of CaR decreased in a dose-dependent manner (Figure 5A). The graph in Figure 5A shows averaged results for 3 independent experiments, and demonstrates a significant decrease in CaR protein as dorfin protein is increased.

When CaR cDNA was transfected into HEK293 cells with increasing amounts of the dominant negative DCT-EGFP cDNA, CaR protein in cell lysates increased as a function of DCT protein (Figure 5B, top blot). The graph illustrates averaged results from 3 independent experiments (Figure 5B). To confirm that EGFP made no contributions to the observed responses, a DCT construct containing a carboxyl terminal *c-myc* epitope was also generated. DCT-*c-myc* protected CaR against dorfin-mediated degradation in a manner comparable to DCT-EGFP (data not shown), indicating that the dorfin fragment specifically competed with endogenous dorfin to protect against CaR degradation. These results suggest that endogenous dorfin regulates CaR degradation.

To test if dorfin mediates degradation of CaR in a proteasome-dependent manner, the effect of the proteasomal inhibitor MG132 on dorfin-mediated CaR degradation was examined. When cells cotransfected with Flag-CaR and EGFP-dorfin were treated with MG132, the dorfin-dependent decrease of CaR protein level was abrogated (Figure 5C), suggesting that a proteasome-dependent mechanism underlies dorfin-mediated degradation of CaR.

VCP interacts with both CaR and dorfin. Dorfin interacts directly with VCP, an AAA-ATPase proposed to have a role in endoplasmic reticulum-associated degradation (ERAD) of proteins (14). In HEK293 cells transiently transfected with Flag-CaR, an antibody against endogenous VCP immunoprecipitated both Flag-CaR and endogenous dorfin (Figure 6, lane 1). In the absence of Flag-CaR, the anti-VCP antibody pulled down endogenous dorfin (Figure 6, lane 2), as has previously been shown (14). Lower blots of Figure 6 indicate endogenous expression of VCP and dorfin, as well as Flag-CaR in lysates of transfected cells. Since both dorfin and CaR can interact with VCP, it is likely that dorfin-mediated ubiquitination and degradation of CaR is occurring at the ER via a VCP-facilitated ERAD pathway.

All forms of CaR are degraded via the proteasome. If CaR interacts with dorfin and VCP at the ER, it is possible that misfolded or unfolded, immature CaR is targeted for proteasomal degradation by dorfin. To test this possibility, we examined the effects of tunicamycin, an

inhibitor of glucosaminyl-1-phosphate transferase, on the amounts and molecular weights of CaR in the absence or presence of MG132. Treatment with tunicamycin induced the appearance of unglycosylated CaR, with molecular weight of 115 kD (Figure 7A). Two differentially glycosylated forms of CaR were also observed, i.e., bands at molecular weights of 130 kD and 150 kD (Figure 7A), respectively. Previous studies have shown that the 130 kD form of CaR is the ER-localized high mannose-modified receptor, and the 150 kD CaR is the mature receptor at the plasma membrane (6,7). Addition of MG132 dramatically increased the amount of the 115 kD form of CaR (185.3 ± 29.6 % normalized to the amount in the absence of MG132), while the two glycosylated forms of CaR were increased to a lesser extent (130 kD form, 159.2 ± 12.6%; 150 kD form, 131 ± 10.3%) (Figure 7B). All forms of CaR are therefore sensitive to ubiquitination and degradation, although the immature forms of CaR (115 kD) which localize to the ER represent the strongest ubiquitination targets.

To determine whether dorfin-mediated ubiquitination is responsible for proteasomal degradation of the variously processed forms of CaR observed in the presence of tunicamycin, we cotransfected HEK293 cells with Flag-CaR with or without the dorfin dominant negative fragment, DCT, treated cells overnight with tunicamycin, and quantified the abundance of CaR forms on western blots (Figure 7C). As illustrated in the blot and associated graph (average of 3 independent experiments), the presence of DCT had an effect on CaR abundance comparable to addition of MG132 (compare Figure 7B and 7C), suggesting that ubiquitination leading to proteasomal degradation of all forms of CaR is mediated by dorfin.

To determine whether endogenous CaR is subjected to proteasome-dependent degradation in the ER, we tested whether MG132 could alter CaR protein levels in MDCK cells, which express endogenous CaR (24, 25) and endogenous dorfin (data not shown). MG132 significantly increased the tunicamycin-induced immature 115-kD form of CaR in MDCK cells (Figure 7D), suggesting that endogenous CaR is regulated by ERAD, presumably via a dorfin-mediated pathway.

DISCUSSION

The molecular mechanisms underlying the trafficking, targeting and turnover of CaR remain largely unknown. In this study we demonstrate that the E3 ubiquitin ligase dorfin, identified as a binding partner to the intracellular carboxyl terminus of CaR by Y2H screening of a human kidney library, interacts with CaR in HEK293 cells and regulates CaR abundance.

Dorfin contains two RING-finger domains and an In-between RING-finger domain at its amino terminus, through which it interacts specifically with the ubiquitin-conjugating enzymes Ubc7 and Ubc8 (11). In common with other RING domain E3 ubiquitin ligases, the dorfin carboxyl terminus confers specificity for substrate proteins including mutant superoxide dismutase-1 (12) and synphilin-1 (13). The region identified in the initial Y2H screen for CaR carboxyl

terminal binding partners corresponds to the distal carboxyl terminus of dorfin, from residues 561 to 838, further narrowed by directed Y2H screens to residues 660 to 838, implicating the distal carboxyl terminus of dorfin in binding to a range of its target proteins. Dorfin also interacts with VCP through its carboxyl terminus (14). It remains to be determined whether specific interaction motifs can be identified within the dorfin carboxyl terminus, which may aid in identifying additional dorfin targets.

Dorfin has been suggested to have role in the pathology of a variety of neurodegenerative diseases. Dorfin localizes to Lewy bodies in Parkinson's disease and dementia (12,14,26), and in Lewy body-like inclusions in amyotrophic lateral sclerosis (13,14). CaR is expressed in tissues that contribute to maintenance of systemic Ca^{2+} homeostasis, including the parathyroids, kidney, intestine and bones (1), as well as other cell types where its role(s) are less well-defined (27). Our results therefore suggest that dorfin may have more general roles as an E3 ligase in a variety of cells and tissues. Our data support a model in which dorfin mediates ubiquitination and proteasomal degradation of CaR via the ERAD pathway, which suggests that dorfin plays a crucial role in regulating the post-translational level of CaR. It will be of interest to determine whether alterations in CaR protein levels in CaR-related diseases are mediated by dorfin, given that endogenous CaR in MDCK cells is subject to ERAD.

The interactions between CaR and dorfin led us to investigate CaR ubiquitination. Ubiquitinated CaR is not observed in the absence of MG132, suggesting that ubiquitinated CaR is rapidly deubiquitinated or degraded. MG132 increased the overall amount of CaR protein, an effect mimicked by a dominant negative fragment of dorfin, suggesting that dorfin-mediated ubiquitination and proteasomal degradation play a significant role in regulating CaR protein. Ubiquitinated CaR immunoreactivity is observed over a wide range of molecular weights, 150 kD to more than 250 kD, typical of polyubiquitination, a potent signal for degradation (28,29). In addition, single point mutations of intracellular lysine residues to arginine did not significantly reduce CaR ubiquitination, suggesting that CaR is ubiquitinated at multiple lysine residues. Overall, our results demonstrate that CaR is multi/polyubiquitinated, and a target for proteasomal degradation.

Ubiquitination plays multiple roles in GPCR signaling. GPCR ubiquitination can occur in an agonist-induced manner or during receptor biosynthesis. Agonist-induced ubiquitination has been observed for yeast α-factor receptors (30,31), β2-adrenergic (32), chemokine CXCR4 (33), and vasopressin V2 receptors (34). Agonist-induced ubiquitination of GPCRs may regulate endosomal targeting, trafficking to lysosomes after endocytosis, or targeting to proteasomes for degradation (30-34). In addition to GPCRs, proteins which directly associate with GPCRs also undergo agonist-induced ubiquitination, including β-arrestins (32,35) and GRK2 (G protein-coupled receptor kinase 2) (36).

Agonist-independent ubiquitination has been observed for δ–opioid receptors

(37,38), rhodopsin (39,40), TRH receptors (41), and as described in the current report, CaR. Agonist-independent ubiquitination results from ERAD, i.e. misfolded, unfolded or abnormal proteins from the ER are retrotranslocated into the cytoplasm, deglycosylated and degraded by the proteasome (42). VCP is an AAA-ATPase that plays crucial roles in multiple aspects of the ERAD pathway in conjunction with its cofactors, Ufd1 and Ndl4 (16-19,42). Studies indicate that retrotranslocation of ERAD substrates from the ER and delivery to the proteasome is catalyzed by the VCP-Ufd1-Ndl4 complex, which binds first to polypeptide backbone and then the polyubiquitin chains on ERAD substrates. ATP hydrolysis catalyzed by VCP is required to complete retrotranslocation; VCP also chaperones polyubiquitinated proteins to the proteasome for degradation (42). Dorfin interacts with VCP, and has been colocalized with VCP in perinuclear aggresomes, i.e., membrane-free, cytoplasmic inclusions containing misfolded, ubiquitinated proteins (14), strongly suggesting the involvement of dorfin in the ERAD pathway. Immunoprecipitation of VCP with both CaR and dorfin from HEK293 cells supports the notion that CaR and dorfin interact at the ER. ERAD-mediated degradation of CaR is further supported by the observation that the tunicamycin-stabilized, unglycosylated form of CaR is most sensitive to MG132 treatment. The ability of the dominant negative fragment DCT to increase the abundance of all CaR forms demonstrates that proteasomal degradation of CaR is initiated by dorfin-mediated ubiquitination.

CaR is a disulfide linked dimer (1,5,8-10). CaR monomers have a large extracellular domain (ECD) of more than 600 amino acids (1). The ECD harbors 11 potential N-linked glycosylation sites, 8 of which are utilized (1,7). The CaR ECD also contains 19 cysteine residues; mutations at any of 14 cysteine residues abolish or dramatically reduce cell surface expression and/or function (1,9). N-linked glycosylation and disulfide bond formation occurs at the ER during membrane protein biosynthesis (43). Given the complexity of the structure of CaR, it is likely that some fraction of newly synthesized receptors are retained intracellularly for quality control purposes, as has been observed for both wt and mutant forms of CaR by western blotting (5-10); only properly glycosylated, dimerized and folded CaR are transported to Golgi complex and the plasma membrane (5-10). Dorfin may represent a critical step in the quality control mechanism, ensuring that only properly folded CaR exits the ER.

In summary, dorfin regulates ubiquitination and degradation of CaR via a VCP-mediated ERAD pathway. The molecular mechanisms underlying differential sorting of CaR to either the Golgi complex or the ERAD pathway remain to be explored.

ACKNOWLEDGEMENTS

We thank Dr. Klaus Seuwen (Novartis Pharma, AG) for human CaR, Dr. Richard Wojcikiewicz (SUNY Upstate Medical University) for HA-ubiquitin, and the members of the Breitwieser laboratory for helpful discussions. Supported by NIH GM 58578 and funds from the Weis Center for Research (GEB), and the graduate program of the Department of Biology, Syracuse University (YH).

REFERENCES

1. Brown, E.M., and Macleod, R.J. (2001) *Physiol. Rev.* **81**, 239-297
2. Brown, E.M., Gamba, G., Riccardi, D., Lombardi, M., Butters, R., Kifor, O., Sun, A., Hediger, M.A., Lytton, J., and Hebert, S.C. (1993) *Nature* **366**, 575-580
3. Romano, C., Yang, W., and O'Malley K.L. (1996) *J. Biol. Chem.* **271,** 28612-28616
4. White, J.H., Wise, A., Main, M.J., Green, A., Fraser, N.J., Disney, G.H., Barnes, A.A., Emson, P., Foord, S.M., and Marshall, F.H. (1998) *Nature* **386**, 679-6630
5. Bai, M., Trivedi, S., and Brown, E.M. (1998) *J. Biol. Chem.* **273,** 23605-23610
6. Fan, G., Goldsmith, P.K., Collins, R., Dunn, C.K., Krapcho, K.J., Rogers, K.V., and Spiegel, A.M. (1997) *Endocrinology* **138**, 1916-1922
7. Ray, K., Clapp, P., Goldsmith, P.K., and Spiegel, A.M. (1998) *J. Biol. Chem.* **273**, 34558-34567
8. Pace, A.J., Gama L., and Breitwieser G.E. (1999) *J. Biol. Chem.* **274,** 11629-11634
9. Ray, K., Hauschild, B.C., Steinbash, P.J., Goldsmith, P.K., Hauache, O., and Spiegel, A.M. (1999) *J. Biol. Chem.* **274,** 27642-27650
10. Bai, M., Trivedi S., Kifor, O., Quinn S.J., and Brown E.M. (1999) *Proc. Natl, Acad. Sci. U.S.A* **6**, 2834-2839
11. Niwa, J., Ishigaki, S., Doyu, M., Suzuki, T., Tanaka, K., and Sobue, G. (2001) *Biochem. Biophys. Res. Commun.* **281**, 706-713
12. Niwa, J., Ishigaki, S., Hishikawa, N., Yamamoto, M., Doyu, M., Murata, S., Tanaka, K., Taniguchi, N., and Sobue, G. (2002) *J. Biol. Chem.* **277**, 36793-36798
13. Ito, T., Niwa, J., Hishikawa, N., Ishigaki, S., Doyu, M., and Sobue, G. (2003) *J. Biol. Chem.* **278**, 29106-29114
14. Ishigaki, S., Hishikawa, N., Niwa, J., Iemura, S., Natsume, T., Hori, S., Kakizuka, A., Tanaka, K., and Sobue, G. (2004) *J. Biol. Chem.* **279**, 51376-51385
15. Wojcikiewicz, R.J.H. (2004) *Trends. Pharmacol. Sci.* **25**, 35-41
16. Ye, Y., Meyer, H.H., and Rapoport, T.A. (2001) *Nature* **6864**, 652-656
17. Dai, R.M., and Li, C.C. (2001) *Nat. Cell. Biol.* **8**, 740-744
18. Jarosch, E., Taxis, C., Volkwein, C., Bordallo, J., Finley, D., Wolf, D.H., and Sommer, T. (2002) *Nat. Cell. Biol.* **4**, 134-139
19. Robinovich, E., Kerem, A., Frohlich, K.U., Diamant, N., and Bar-Nun, S. (2002) *Mol. Cell.Biol.* **22** 626-634
20. Goldsmith, P.K., Fan, G., Miller, J.L., Rogers, K.V., and Spiegel, A.M. (1997) *J. Bone. Miner. Res.* **12**, 1780-1788
21. Zhang, M., and Breitwieser, G.E. (2005) *J. Biol. Chem.* **280**, 11140-11146
22. Gama, L., and Breitwieser, G.E. (1999) *BioTechniques* **26**, 814-815

23. Gietz, R.D., and Schiestl, R.H. (1995) *Methods Mol. Cell. Biol.* **5**, 255-269
24. Arthur, J.M., Collinsworth, G.P., Gettys, T.W., Quarles, L.D., and Raymond, J.R. (1997) *Am. J. Physiol. Renal. Physiol.* **273**, F129-F135
25. Arthur, J.M., Lawrence, M.S., Payne, C.R., Rane, M.J., and McLeish, K.R. (2000) *Biochem. Biophys. Res. Commun.* **275**, 538-541
26. Hishikawa, N., Niwa, J., Doyu, M., Ito, T., Ishigaki, S., Hashizume, Y., and Sobue, G. (2003) *Am. J. Pathol.* **163**, 609-619
27. Peace, S.H.S., and Thakker, R.V. (1997) *J. Endocrinol.* **154**, 371-378
28. Pickart, C.M. (2001) *Annu. Rev. Biochem.* **70**, 503-533
29. Weissman, A.M. (2001) *Nat. Rev. Mol. Cell Biol.* **2**, 169-178
30. Roth, A.F., and Davis, N.G. (1996) *J.Cell Biol.* **134**,661-674
31. Hicke, L. and Riezman, H. (1996) *Cell* **84**, 277-287
32. Shenoy, S.K., McDonald, P.H., Kohout, T.A., and Lefkowitz, R.J. (2001) *Science* **294**, 1307-1313
33. Marchese, A., and Benovic, J.L. (2001) *J. Biol. Chem.* **276**,45509-45512
34. Martin, N.P., Lefkowitz, R.J., and Shenoy, S.K. (2003) *J. Biol. Chem.* **278**, 45954-45959
35. Shenoy, S.K., and Lefkowitz, R.J. (2003) *J. Biol. Chem.* **278**, 14498-14506
36. Penela, P., Ruiz-Gomez, A., Castano, J.G., and Mayor, F.J. (1998) *J. Biol. Chem.* **273**, 35238-35244
37. Petaja-Repo, U.E., Hogue, M., Laperriere, A., Bhalla, S., Walker, P., and Bouvier, M. (2001) *J. Biol. Chem.* **276**, 4416-4423
38. Chaturvedi, K., Bandari, P., Chinen, N., and Howells, R.D. (2001) *J. Biol. Chem.* **276**, 12345-12355
39. Saliba, R.S., Munro, P.M.G., Luthert, P.J., and Cheetham, M.E. (2002) *J. Cell Sci.* **115**, 2907-2918
40. Illing, M.E., Rajan, R.S., Bence, N.F., and Kopito, R.R. (2002) *J. Biol. Chem.* **37**, 34150-34160
41. Cook, L.B., Zhu, C.C., and Hinkle, P.M. (2003) *Mol. Endocrinol.* **17**, 1777-1791
42. Meusser, B., Hirsch, C., Jarosch, E., and Sommer, T. (2005) *Nat. Cell. Biol.* **7**, 766-772
43. Kostova, Z., and Wolf, D.H. (2003) *EMBO Journal* **22**, 2309-2317

ABBREVIATIONS

The abbreviations used are: CaR, calcium sensing receptor; CT, carboxyl terminus; DCT, dorfin carboxyl terminal dominant negative fragment; ER, endoplasmic reticulum; ERAD, endoplasmic reticulum-associated degradation; GPCR, G protein-coupled receptor; VCP, valosin-containing protein; HEK293, human embryonic kidney 293; MDCK, Madin-Darby canine kidney; EGFP, enhanced green fluorescence protein; PBS, phosphate-buffered saline; RING, really interesting new gene; Y2H assay, yeast two-hybrid assay

FIGURE LEGENDS

Figure 1. Analysis of interaction sites on calcium-sensing receptor (CaR) and the E3 ubiquitin ligase dorfin by directed Y2H assay. (A). Schematic representation of CaR and localization of the interaction site for dorfin carboxyl terminal fragment (residues 561-838). The cytoplasmic carboxyl terminus of CaR (residues 866 to 1078) was truncated from both the amino and carboxyl termini as indicated, and screened by cotransformation of the AH109 yeast strain with the CaR fragment plus the carboxyl terminal of dorfin (residues 561-838). TM, transmembrane heptahelical domain; ECD, extracellular domain. (B). Schematic representation of dorfin and localization of the interaction site for CaR carboxyl terminal fragment (residues 866-1078). Truncations were generated from both the amino and carboxyl terminal ends of the dorfin fragment (residues 561-838) and screened by cotransformation of the AH109 yeast strain with the dorfin fragment plus the carboxyl terminus of CaR (residues 866-1078). R1, R2, RING finger domains; IBR, in between RING-finger domain. For (A) and (B), positive interactions, resulting in activation of three reporter genes (HIS3, ADE2 and MEL1) are indicated as +.

Figure 2. Interaction of full length CaR and dorfin in HEK293 cells. (A). HEK293 cells were transfected with (lane 1) or without (lane 2) Flag-CaR cDNA. Cells were harvested 72 hours after transfection. Anti-Flag antibody was used to immunoprecipitate samples, and blots were probed with anti-dorfin antibody D-30 (top panel). Lysates were probed with anti-dorfin D-30 antibody (middle panel) or anti-CaR LRG antibody (bottom panel) to assess protein expression. (B). Flag-CaR cDNA transfected HEK293 cells were cotransfected with EGFP-dorfin (lane 1), DNT-EGFP (lane 2) or DCT-EGFP (lane 3), respectively. Anti-Flag antibody was used to immunoprecipitate samples, and blots were probed with anti-GFP antibody (top panel). Lysates were probed with anti-GFP antibody (middle panel) or anti-CaR LRG antibody (lower panel) to assess protein expression.

Figure 3. Ubiquitination of CaR in HEK293 cells. (A). Flag-CaR or Flag-CaR(0K) cDNA was transfected into HEK293 cells with HA-Ub cDNA. Cells were incubated without (lanes 1, 3) or with (lanes 2, 4) 10 μM proteasomal inhibitor MG132 for 12 hrs prior to lysis. Cell lysates were immunoprecipitated with anti-Flag antibody and the precipitated pellets were treated with 1% SDS/PBS to disrupt non-covalent interactions. Supernatants were diluted with lysis buffer, followed by a second immunoprecipitation using anti-Flag antibody. The blot was probed with anti-HA antibody (upper panel). The same blot was then stripped and probed with anti-CaR antibody LRG (lower panel). (B). Flag-CaR cDNA or Flag-CaR(0K) cDNA was transfected into HEK293 cells. Cells were preincubated with 0.5 mM Ca^{2+} overnight prior to exposure to either 0.5 or 5 mM Ca^{2+} for 10 min (37°C), followed by immunoblotting of lysates with anti-phospho-ERK1/2 antibody. (C). Flag-CaR cDNA or Flag-CaR(0K) cDNA was transfected into HEK293 cells. Anti-Flag antibody was used to immunoprecipitate samples, and blots were probed with anti-dorfin D-30 antibody (top blot). Lysates were probed with anti-dorfin D-30 antibody (middle blot) or anti-CaR LRG antibody (bottom blot).

Figure 4. Regulation of CaR ubiquitination by dorfin. (A). Dorfin mediates ubiquitination of CaR. Flag-CaR (3 μg) and HA-Ub (2 μg) cDNAs were cotransfected into HEK293 cells, without (-) or with (+) EGFP-dorfin cDNA (6 μg). Cells were incubated with 10 μM MG132 for 12 hrs prior to lysis. Cell lysates were immunoprecipitated with anti-Flag antibody and blots probed with anti-HA antibody. CaR ubiquitination was quantified and normalized to basal ubiquitination in the absence of exogenous dorfin; significance at * $p < 0.05$. (B). Dominant negative dorfin fragment DCT inhibits ubiquitination of CaR. Flag-CaR cDNA (3 μg) and HA-ubiquitin cDNA (2 μg) were cotransfected into HEK293 cells, without (-) or with (+) DCT-EGFP cDNA (6 μg). Methods as described in (A).

Figure 5. Regulation of steady-state protein level of CaR by dorfin. (A). Wild-type dorfin enhances degradation of CaR. Flag-CaR cDNA (1 μg) was transfected into HEK293 cells with increasing amounts of EGFP-dorfin cDNA (0, 2, 4, or 6 μg). Cell lysates were probed for Flag-CaR, endogenous actin and EGFP-dorfin by immunoblotting with anti-CaR (LRG), anti-actin, or anti-GFP antibodies. Graph (average of 3 independent experiments) indicates normalized CaR protein or EGFP-dorfin as a function of transfected EGFP-dorfin cDNA. CaR protein was normalized to amount in the absence of exogenous EGFP-dorfin; EGFP-dorfin normalized to that observed at 6 μg EGFP-dorfin cDNA. Filled circles, Flag-CaR; open circles, EGFP-dorfin. (B). Dominant negative construct of dorfin (DCT-EGFP) stabilizes CaR. Flag-CaR cDNA (1 μg) was transfected into HEK293 cells with increasing amounts of DCT-EGFP cDNA (0, 2, 4, or 6 μg). The remaining procedures were described in (A). Graph (average of 3 independent experiments) indicates normalized CaR protein or DCT-EGFP, normalized as described in (A). Filled circles, Flag-CaR; open circles, DCT-EGFP. For both (A), (B), significance at * $p < 0.05$. (C). Flag-CaR cDNA (1 μg) was transfected into HEK293 cells without (lane 1) or with EGFP-dorfin (6 μg) (lanes 2 and 3). Cells were treated without (lanes 1 and 2) or with (lane 3) MG132 for 12 hours before lysis. Cell lysates were probed for Flag-CaR by immunoblotting with anti-CaR LRG antibody.

Figure 6. VCP/CaR/Dorfin coimmunoprecipitation in HEK293 cells. HEK293 cells were transfected without (-) or with (+) Flag-CaR cDNA. Cell lysates were immunoprecipitated with anti-VCP antibody and western blots probed with anti-CaR antibody LRG (first blot). The same blot was stripped and reprobed with anti-dorfin antibody D-30 (second blot). The expression of endogenous VCP, transfected CaR, and endogenous dorfin were confirmed by immunoblotting cell lysates with anti-VCP antibody (third blot), anti-CaR LRG antibody (fourth blot), or anti-dorfin D-30 antibody (fifth blot).

Figure 7. Sensitivity of immature forms of CaR to proteasomal degradation. (A). Tunicamycin stabilizes an immature form of CaR. HEK293 cells transfected with Flag-CaR cDNA were treated without or with tunicamycin (5 μg/ml) for twelve hours prior to lysis. Lysates were immunoprecipitated with anti-Flag antibody and probed with anti-CaR LRG antibody. (B). MG132 increases the amounts of immature forms of CaR. HEK293 cells were transfected with Flag-CaR and HA-Ub cDNAs, and incubated with tunicamycin (5 μg/ml) without or with MG132 (10 μM), for 12 hrs prior to lysis. Lysates were immunoprecipitated with anti-Flag antibody and probed with anti-CaR LRG antibody. Three forms of CaR are

evident in tunicamycin, 1, fully glycosylated CaR (150 kD); 2, ER-resident high-mannose CaR (130 kD); 3, unglycosylated CaR (115 kD). The amount of CaR protein in each form was quantified in the absence or presence of MG132, and average results for 3 independent experiments are illustrated (each band normalized to the amount observed in the absence of MG132), significance at * $p < 0.05$. (C). DCT increases the amounts of immature forms of CaR. HEK293 cells were transfected with Flag-CaR without or with DCT-EGFP. Cells were incubated with tunicamycin (5 mg/ml) for 12 hrs prior to lysis. Experiments as in (A). Graph indicates amounts of 3 forms of CaR protein in the absence or presence of DCT-EGFP, normalized to the amount in the absence of DCT-EGFP. Significance at * $p < 0.05$. (D). MG132 increases the amounts of immature CaR in MDCK cells. MDCK cells were treated with tunicamycin (5 μg/ml) without or with MG132 (10 μM) for 12 hrs prior to lysis. Lysates were immunoblotted with anti-CaR LRG antibody.